

# Substantial Doppler broadening of atomic-hydrogen lines in DC and capacitively coupled RF plasmas

Kamran Akhtar<sup>1</sup>, John E. Scharer<sup>2</sup>, and Randell L. Mills<sup>3</sup>  
<sup>1,3</sup> BlackLight Power, Incorporated  
493 Old Trenton Road, Cranbury, New Jersey 08512

<sup>2</sup>Department of Electrical and Computer Engineering  
University of Wisconsin-Madison, Wisconsin 53706

## Abstract

The mechanism of extraordinary broadening of the Balmer lines of hydrogen admixed with noble gases in a DC glow discharge and a capacitively coupled rf discharge is studied over a wide range of pressure and gas compositions to test the field acceleration model [Cvetanovic et. al. J. App. Phys., Vol. 97, 033302-1, 2005]. High-resolution optical emission spectroscopy is performed parallel to the electrode axis (end-on) and perpendicular to the electrode axis (side-on) along with Langmuir probe measurements of plasma density and electron temperature for the parallel plate RF capacitive discharge case. Sharp pin-shaped tungsten DC electrodes are also used to minimize the backscattering of ions that are theorized by a field acceleration model to be heated in the sheath region. An excessively broad and symmetric (Gaussian) Balmer emission line corresponding to 20-60 eV of hydrogen atom energy is observed in Ar/H<sub>2</sub> and He/H<sub>2</sub> plasmas when compared to the majority species atom temperatures. Energy is transferred selectively to hydrogen atoms whereas the atoms of admixed He and Ar gases remain cold (<0.5 eV). Since there is neither a preferred ion nor atom in the field acceleration model, one should also observe enhanced temperature hydrogen and helium atoms in He/H<sub>2</sub> discharges where the atomic mass is more comparable (4:1).

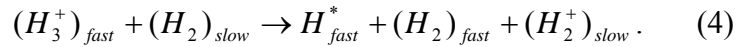
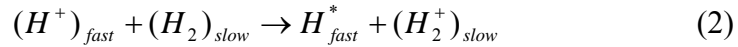
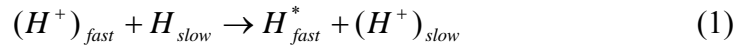
## I. INTRODUCTION

Substantial Doppler broadening of hydrogen Balmer lines has been observed in pure hydrogen and specific gaseous mixtures of hydrogen with certain heavier atom plasmas produced by DC and capacitively coupled 13.56 MHz radio frequency waves [1-17]. This broadening is caused by the presence of excited hydrogen atoms. Historically, most mechanisms proposed for excessive  $H_\alpha$  broadening in pure hydrogen and mixtures of hydrogen with inert gases [1-14] are explained in terms of energetic ions ( $H^+$ ,  $H_2^+$  and  $H_3^+$ ) that are accelerated in the cathode fall region followed by energy transfer to the matrix gas (H and  $H_2$ ) through charge exchange collisions. However, there are variations in the proposed theoretical explanations of the mechanisms that provide energy to atomic H and cause the observed enhanced blue-shifted  $H_\alpha$  spectra width that is symmetric with respect to the red-shifted portion of the emission profile. It should be noted, however, that none of these mechanisms explains the selective transfer of energy to the hydrogen atomic state with the atoms of the admixed gases remaining cold ( $<0.5$  eV) even when the mass ratios are comparable.

In a pure hydrogen discharge, the Doppler-broadened profile exhibits the presence of a bimodal (or a tri-modal) distribution of neutral species temperatures [14]. The profile consists of a central peak that corresponds to slow thermal hydrogen atoms with kinetic energies in the range 0.25 to 1 eV. The population of warm H atoms (10-20 eV) is evident in the plateau of the Doppler broadened profile along with a population of fast hydrogen atoms ( $> 40$  eV). There is general agreement on the mechanisms proposed for the production of slow H ( $\sim 0.1$ -1eV) atoms in the excited  $n=3$  state through the process

of dissociative excitation,  $H_2 + e^- \rightarrow H_2^* + e^- \rightarrow H^*(n=3) + H$ , and dissociative ionization,  $H_2 + e^- \rightarrow 2e^- + H_2^+ \rightarrow H^*(n=3) + H^+$ , of hydrogen molecules and electron impact excitation of H atoms,  $H + e^- \rightarrow e^- + H^*(n=3)$  [1-2].

There are significant variations in the literature describing the mechanisms proposed to explain the production of hydrogen atoms with energies greater than 20 eV. These were originally proposed to be the result of dissociation of  $H_2^+$  ions in vibrationally excited molecular ground states [2-3]. Recently, the mechanism of charge exchange between ions accelerated in the sheath and neutrals and ion impact on electrodes has been proposed as the source of energetic hydrogen atoms in these discharges. In this model, henceforth called the Collisional Model (CM) [5 and references therein], sheath accelerated  $H^+$  and  $H_3^+$  ions in a hydrogen plasma are proposed to either transfer charge directly to the hydrogen atom or dissociate the  $H_2$  molecule followed by charge exchange collisions to explain the energy spectrum of hydrogen atoms [1-15]. The processes are governed by the following reactions [5-7] where the \* indicates the excited n=3 atomic state:



Since the particle acceleration due to the electric field is directional, the energy gained by a positive ion as it travels towards the cathode will maintain that directionality along with the directed energy of the excited hydrogen atom as long as ion-neutral collision rates are

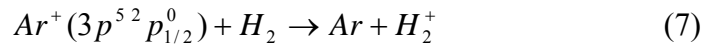
sufficiently small that is the case at our lower pressures of 10-100 mTorr. This mechanism can only account for the red portion of the spectrum when viewed optically towards the ion accelerating electrode sheath. The observed symmetry in the Gaussian profile of the hydrogen Balmer line is explained in terms of the sputtered fast H atoms and the back-reflected fast H atoms from the cathode surface [5]. It is argued that this will give rise to a symmetric distribution of energetic H atoms leaving the cathode compared to those accelerating towards the cathode. If ion-neutral collisions are infrequent such as is the case for our lowest pressures of 10 mTorr, one should also see a much lower alpha heating perpendicular to the electrode axis. To test these principles, we have constructed a new DC glow discharge with sharply tapered tip electrodes to decrease the effective surface area and minimize the theoretically proposed, back-reflected flux of fast H atoms that could give rise to the symmetric  $H_\alpha$  broadening spectrum. We also vary the concentrations of  $H_2$  and noble gases over a wider pressure range (10 mTorr-10 Torr) than has been previously examined to examine the effects of ion-neutral charge exchange processes on the Balmer emission lines.

In the presence of noble gases, the additional process of charge transfer has been proposed to explain the symmetric  $H_\alpha$  broadening [3,12-13]. The introduction of Ar in a pure  $H_2$  plasma increases the Balmer line emission intensity and indicates that the concentration of excited hydrogen atoms in the excited  $n=3$  state is also increased. In addition, the fractional population of hot hydrogen atoms obtained from the area under the Gaussian curve implies a concentration in excess of 80 percent of the total population in the excited  $n=3$  state. It has been suggested in the above articles [3] that energetic  $Ar^+$  ions dissociate and ionize  $H_2$  to form  $ArH^+$  that enhances the population of  $H_3^+$  that is

proposed as the primary source of atomic hydrogen as shown below when Eq. (6) is combined with Eq. (4).



The role of metastable argon ions in the enhanced production of  $H_3^+$  ions through the formation of molecular hydrogen ions has also been emphasized [6].



It has been suggested [3] that the contribution of these pathways to the significant production of  $H_3^+$  in Ar/H<sub>2</sub> results in an enhanced population of energetic H<sub>fast</sub> atoms through the processes described in Eqns. (3-4). It should be noted that none of these proposed mechanisms fully explains the entire energy spectrum of H atoms observed in these experiments.

However, some of the recent observations [17-26] in DC and capacitively coupled rf discharges are in contrast to the field acceleration based Collisional Models (CM) described earlier. For example, it is important to note that, to the best of our search of the scientific literature, no experimental observation has ever been reported, including results in this paper where equally energetic atoms of admixed gases have been found even when the plasma is collisional and ion mass ratios are comparable (e.g. He/H<sub>2</sub> plasmas with mass ratio of 4:1). The energy is transferred selectively only to the hydrogen atom whereas the electron temperature is less than few eV and admixed gas atoms remain cold (<0.5 eV). Since the radiative life time of n=3 state is short (10<sup>-8</sup> s), the observation of

comparably hot hydrogen atoms in regions far outside the plasma sheath(10-15 cm) requires the local creation of energetic H atoms.

In order to test the validity of field acceleration based Collisional Model (CM) [5] to explain  $H_{\alpha}$  broadening in hydrogen plasmas and plasmas of hydrogen admixed with noble gases, this paper discusses comprehensive experiments that cover a wider range of gas pressure and plasma parameters than is currently available in the literature. A DC glow discharge with tapered pin-shaped electrodes to minimize hydrogen atom back reflections along the electrode axis that are part of the CM and a capacitively coupled parallel plate radio frequency plasma are utilized. Experiments are conducted over a wide pressure range along with a wide range of different hydrogen-noble gas mixture ratios. Both parallel and perpendicular spectral observation angles are used to test the ability of the CM to explain the unusual nature of the observed hydrogen broadening. The CM mandates that observations parallel and perpendicular to the electric field lines will yield different emission profiles at different angles of observation if the collisional scattering rate is sufficiently small that can occur in our experiments at the lower 10 mTorr pressures. In addition, the presence of hot H atoms was examined in regions far away (10-20 cm) from the high electric field plasma sheath region near the electrodes. In addition to plasma emission spectroscopy, a Langmuir probe is also used to diagnose the density and thermal electron temperatures for the capacitive discharge plasma.

## II. EXPERIMENTAL SYSTEM

The experimental arrangement for the DC discharge is shown in Fig. 1. In this new configuration, the discharge is created between fine tips of 2% thoriated tungsten

electrodes of diameter 1/8 inch spaced 2 cm apart inside either a 1/2 inch or 1 inch diameter quartz tube. Very fine electrode tips (Fig.1) that are tapered over the last 1/2 inch to a point are used to minimize the surface area perpendicular to the face of the electrodes to greatly reduce the backscatter process that the CM uses to explain the symmetry in the  $H_{\alpha}$  broadening. The high E-field near the sharp electrode tip will reduce rapidly as one moves away from it due to plasma sheath effects. High-resolution plasma emission spectroscopy is performed through an annulus parallel to the electrode axis along the electric field lines (end-on) and perpendicular to the field lines (side-on). For the end-on observation, plasma emission can be sampled looking towards the anode or cathode. For the side-on observation, an axial scan of the plasma emission is observed in a region adjacent to the cathode rod. Here the cathode tip is located at  $z=0$  cm. The DC plasma setup is placed on an X-Y motion table so that an accurate axial measurement can be carried out without changing the position of the fiber optic bundle. The discharge pressure is maintained in the range from 10 mTorr to 10 Torr. A stabilized negative DC power supply (Kaiser System Inc., Beverly, MA) with voltage and current in the range 0-2000 V and 0-500 mA, respectively, is used to create the plasma. A high wattage ballast resistor of 20 k $\Omega$  is used in series with the power supply to limit the discharge current. Once the discharge is created, the glow discharge is maintained with cathode-anode voltages of 300-400 volts and results in discharge currents  $\sim$ 10 mA, depending upon the gas pressure, gas flow and discharge configuration.

The capacitively driven radio frequency plasma system consists of a large cylindrical (14 cm ID  $\times$  36 cm length) quartz plasma chamber with two electrodes (stainless steel plates of diameter 8.25 cm) placed 1 cm apart at the center (Fig. 2). Radio

frequency power (13.56 MHz, RF Power Products Inc. NJ, Model RF 5, 500 Watts) is coupled to the electrode using a commercially available impedance matching network (RF VII Inc., Glassboro, NJ). Radio frequency power from the source is fed through the impedance matchbox to the capacitive electrodes using a 1/2-inch diameter steel tube that also facilitates the end-on (parallel to the electric field) observation of plasma through holes in the center of the electrodes. One of the electrodes is permanently grounded. A common ground is maintained for the grounded electrode, rf shield and vacuum system. Two ports in the center of the plasma chamber (Position 2) permit side-on observations of plasma emission  $90^\circ$  and  $45^\circ$  to the electric field. Another side port at the same position allows insertion of a Langmuir probe for plasma density and electron temperature measurements. Plasma emission far away (15 cm) from the high-field plasma sheath region is sampled at Positions 1 and 2. In order to ensure that the plasma emission sampled at positions 1 and 2 have no contribution from light reflected from the inside of the rf shield enclosure, a non-reflecting coating is placed inside the rf shield.

A helium leak detector (QualyTest, Model: HLT 260, Pfeiffer Vacuum) is utilized to leak test the evacuated plasma chamber. The plasma chamber is maintained with a leak rate below  $10^{-7}$  Torr-L/s. Independent mass flow controllers (MKS) were used to introduce UHP grade (99.999%)  $H_2$ , Ar, He and Xe gases into the plasma chamber through Ultratorr fittings at one end. The chamber pressure for all gas compositions is maintained between 10 mTorr and 10 Torr with flow rates in the 20-30 sccm range. An MKS Baratron gauge is used to read the chamber pressure.

### III. DIAGNOSTICS

## A. Plasma Emission Spectroscopy

Plasma emission from the glow discharge passes through a high-quality UV (200-800 nm) fiber-optic bundle into a monochromator through a 220F matching fiber adapter that is detected either by a photomultiplier tube (PMT) with a stand-alone power supply of 995 volts or by a high quality scientific grade liquid nitrogen cooled CCD array. The numerical aperture of the fiber optic bundle is 0.12 and the corresponding acceptance angle is  $12^\circ$ . The spectrometer utilizes a 1250 mm focal length spectrometer (Jobin Yvon Horiba: Model 1250M Research Spectrometer) with a 2400 g/mm grating and a high resolution of  $\pm 0.006$  nm. The spectrometer is rated for an accuracy of  $\pm 0.05$  nm and repeatability of  $\pm 0.005$  nm. The spectrometer was scanned through emission profiles of Balmer lines with a step size of 0.01 nm. The entrance and exit slits were set at 20  $\mu\text{m}$ . The liquid nitrogen cooled Symphony model CCD detectors are a family of array detectors from Jobin Yvon with 16 bit ADC with 20 KHz and 1 MHz read out. A back illuminated 2048 $\times$ 512 CCD of 13.5  $\mu\text{m}$   $\times$  13.5  $\mu\text{m}$  size provides very high-resolution capability.

The Doppler-broadened line shapes for atomic hydrogen have been used to calculate the energy of the atomic hydrogen. The motion of a radiating particle moving towards or away from an observer results in a wavelength shift of the emitted line. This broadening is related to the random thermal motion of the emitting atoms and for a Maxwellian velocity distribution it depends only on the translational (kinetic) temperature. The full half-width,  $\Delta\lambda_G$ , of the Gaussian profile results from the Doppler ( $\Delta\lambda_D$ ) and instrumental ( $\Delta\lambda_I$ ) half-widths are  $\Delta\lambda_G = \sqrt{\Delta\lambda_D^2 + \Delta\lambda_I^2}$ . In order to calibrate the instrument half-width when the CCD of finite pixel spectral width is utilized, the line

width of 546 nm Hg I line from NIST calibrated mercury lamp was measured. The slit width was kept constant at 20  $\mu\text{m}$ . The measured half-width 0.006 nm is negligible. The temperature of atomic hydrogen in terms of the Doppler ( $\Delta\lambda_{\text{D}}$ ) half-width is given as [29]

$$\Delta\lambda_{\text{D}} = 7.16 \times 10^{-7} \lambda_0 \left( \frac{T}{\mu} \right)^{1/2} \text{ nm.}$$

Here  $\lambda_0$  is the line wavelength in nm, T is the temperature in K, and  $\mu$  is atomic mass number (=1 for hydrogen). It can be seen that Doppler broadening is more pronounced for lighter elements at high temperatures. For high densities  $>10^{13}/\text{cc}$ , Doppler broadening competes with Stark broadening. In addition, a contribution to the broadened profile may arise from the mass motion of the plasma. However, for these glow discharges where the plasma density is low ( $<10^{11}/\text{cc}$ ), the contribution of Stark broadening to the line shape profile can be neglected without loss of accuracy. We checked the contribution from the mass motion of the plasma by sampling the plasma emission side-on as well as end-on. The absence of line shift shows that the line broadening is primarily due to the thermal motion. In each case, the error in the average Doppler half-width over 10 scans was about  $\pm 5\%$  that is attributed to the fluctuations in the plasma. The half-width of the Doppler broadened emission profile was obtained using a multi-Gaussian curve fit utilizing the curve fitting software GRAMS from Jobin Yvon Horiba.

## B. Plasma Density Measurement

In the present work, Langmuir probe (LP) data has been used to obtain the bulk plasma density and thermal electron temperature in the capacitive discharge [30-32]. The

cylindrical Langmuir probe is a tungsten tip of radius 1 mm and length 5 mm enclosed in an alumina tube. The LP is placed between the electrodes at position 2 about 2 cm inside the Pyrex chamber where most of the plasma heating occurs. In order to characterize the capacitively coupled radio frequency plasma, an rf compensated [31] LP is utilized that allows accurate measurement of bulk electron temperature. The probe filtering does not allow time varying, non-Maxwellian properties of the electron energy distribution to be readily observed. However, a small fraction (less than 1%) of fast electrons ( $\sim 10\text{-}15$  eV) have been observed in capacitively coupled discharges where bulk electron temperatures are only few eV [33-35].

Data acquisition software written in Lab View is used for automatic transfer from the oscilloscope to the computer. The entire LP data analysis in the present work was undertaken using an interactive graphics based software package developed in MatLab.

#### IV. EXPERIMENTAL RESULTS

##### A. DC Discharge

The axial profile of the Balmer  $H_\alpha$  line (near 656.3 nm) observed perpendicular (side-on) and parallel to the electrode axis (end-on) looking towards anode as well as cathode is obtained for Ar/H<sub>2</sub> (95/5%), He /H<sub>2</sub> (95/5%), and Xe/H<sub>2</sub> (95/5%) 300-400 V DC plasmas produced between fine tipped electrodes spaced 2 cm apart. The DC discharge is produced over a wide pressure range (and ion mean free path) from 10 mTorr-10 Torr. Significant  $H_\alpha$  broadening was observed in Ar/H<sub>2</sub> and He/H<sub>2</sub> plasmas whereas no broadening was observed for Xe/H<sub>2</sub> plasmas.

Axial profiles of the  $H_{\alpha}$  line for side-on as well as for end-on observations for argon mixed with 5% hydrogen plasma are isotropic and symmetric over entire pressure range from 10 mTorr to 10 Torr. Typical side-on and end-on emission profiles for 1 Torr of argon mixed with 5% hydrogen are shown in Fig. 3 and Fig. 4, respectively. The axial scan is performed parallel to the cathode pin axis with the tip located at  $z=0$ . The fiber optic cable entrance aperture is placed perpendicular to the surface of the quartz tube. The sampled plasma volume with an acceptance angle of  $12^{\circ}$  for 1 inch and  $\frac{1}{2}$  inch diameter tubes is  $30 \text{ mm}^3$  and  $4 \text{ mm}^3$ , respectively. The  $H_{\alpha}$  line profiles clearly exhibit a two-component Doppler-broadened profile corresponding to two populations of hydrogen atoms. The central narrow part corresponds to slow hydrogen atoms with temperatures in the range of 0.4-0.5 eV. The broad component of the profile corresponds to fast hydrogen atoms with an average temperature of  $\sim 40$  eV. The fractional concentration of the slow part as obtained by curve fitting is 20-25% and the fast hydrogen component corresponds to 80-75 % indicating that the production of fast hydrogen atoms is substantial. It should be noted here that the fractional concentration of fast excited H atoms is given by the ratio of area under the broad Doppler profile to the total area under the emission profile. Similar emission profiles are obtained for He/ $H_2$  plasmas where the fast hydrogen atoms have temperatures in the range of 30-40 eV. In contrast, only the slow component ( $\sim 0.5$  eV) of the hydrogen population is observed for Xe/ $H_2$  plasmas (Fig. 5). The axial temperature and population profiles of both fast and slow hydrogen atoms corresponding to the emission profiles in Fig. 3 are shown in Fig. 6. It can also be seen from Figs. 3 and 6 that the average width of the two Gaussians of the Doppler broadened profile and hence the average temperature does not change appreciably along the axis. Even though the

potential drops primarily near the cathode tip, the population of fast hydrogen atoms (area under the curve) peaks at a distance 2 cm away from the cathode tip. Moreover, the population of fast hydrogen atoms in  $n=3$  excited state as a fraction of the total population is a minimum (82%) at the cathode tip ( $z=0$ ) and it increases to 94% at  $z = 2$  cm and remains nearly uniform up to  $z = 8$  cm (Fig. 6). It is noted that the intensity and corresponding plasma density decreases away from the cathode tip (Fig. 3) although the hot hydrogen component fraction increases.

Figure 7 shows the normalized emission profile for an end-on observation in Ar/H<sub>2</sub> and He/H<sub>2</sub> plasmas at 1 Torr looking towards the anode. A similar symmetrical emission profile is also obtained when the emission is sampled looking towards the cathode. Reflection of field-accelerated ions in equal measure relative to the accelerated direction is required by the CM to explain the absence of either a predominant red or blue wing in the emission profile for the end-on observation. Furthermore, the symmetrical profile cannot be explained by the gas matrix collision effect as very little change in the normalized emission profile symmetry is observed as the gas pressure is varied from 10 mTorr to 10 Torr resulting in a variation of electron-neutral collision frequencies and charge exchange mean free path by three orders of magnitude (Fig. 8).

Figure 9 shows the change in H <sub>$\alpha$</sub>  broadening as fractional concentration of admixed noble gas is varied. Thermal energy of hot hydrogen atom increases with increasing concentration of Ar and He and decreases with Xe concentration. In addition, the transfer of energy from the electric field in these admixed plasmas is selectively to hydrogen atoms. Since the mass ratio of He to atomic hydrogen is 4:1, especially for highly collisional plasmas at higher gas pressures, it is expected from the Collisional

Model [5] that a correspondingly energetic concentration of helium atoms (Doppler broadened profile) will be present. The Doppler half-width of the 667.82 nm He I line as shown in Fig. 10 is 0.012 nm and it can be accurately resolved by the high-resolution spectrometer with an instrumental half-width of only 0.006 nm. The He atoms' average thermal energy corresponding to a 0.012 nm Doppler half-width is 0.2 eV. No change in Doppler broadening of the 667.82 nm He I line was observed for all pressure and composition ranges studied in these experiments. The absence of hot helium atoms in He/H<sub>2</sub> plasmas where the hydrogen atoms have 30-40 eV energies also contradicts the Collisional Model because the atomic mass ratios are comparable (4:1).

#### B. Capacitively Coupled RF Discharge

The capacitively coupled radio frequency discharge is characterized using Langmuir probe (LP) and plasma emission spectroscopy diagnostics. The LP is employed to measure electron bulk plasma density ( $n_e$ ) and the bulk thermal electron temperature ( $T_e$ ). An rf filter compensated detection is employed [31] to eliminate the effects of rf on the probe measurements. Researchers [33-35], have reported only small (less than 1 %) concentrations of fast (10-15 eV) electrons produced in capacitive discharges in certain configurations. These concentrations can only provide ionization and excitation of atoms and cannot account for the strong H $_{\alpha}$  heating observed in these experiments. In addition, the fast electron ionization mean free path in argon at 100 mTorr [36] at 20 eV is 0.05 cm for these plasmas. Thus, fast electrons created near the electrodes cannot contribute to ion energetics far from the electrodes.

A side port at position 2 (Fig. 2) allows the insertion of the LP between the rf electrodes. The on-axis LP measurements are summarized in Table 1 for different noble gases admixed with 10% hydrogen at constant pressure of 100 mTorr. The coupled radio frequency power is maintained constant at 100 W for all the cases. In general, a low-density plasma ( $\sim 10^{10} \text{ cm}^{-3}$ ) with bulk electron temperatures of 2-3 eV is observed for all plasma conditions. There is a slight drop ( $\sim 15\text{-}20\%$ ) in  $n_e$  as well as in  $T_e$  as hydrogen is added to the pure noble gas plasmas.

$H_\alpha$  emission from capacitively coupled rf discharges that are varied over a 10 mTorr-10 Torr pressure range is sampled perpendicular to the electric field between the large disc electrodes (Position 2 in Fig. 2) and along the electric field through the 1 cm holes in the electrode plates (end-on). In addition, observations are also made at locations far way from the electrode plates (Positions 1 and 3 in Fig. 2). Isotropic and symmetric  $H_\alpha$  line profiles are observed for all three locations, independent of the observation angle relative to the electric field direction. The line profile also remains symmetric as the gas pressure is varied over a wide range from 10 mTorr to 10 Torr. Line broadening is observed only for Ar/ $H_2$  and He/ $H_2$  plasmas and the energy of the hot H atoms increases with increasing concentration of Ar and He gases whereas it decreases with Xe concentration. For the Ar/ $H_2$  and He/ $H_2$  plasmas, the energy is selectively transferred to the hydrogen atoms. In addition, the temperature of fast H atoms is observed to be uniform and isotropic throughout the plasma chamber.

The average thermal energy of hot hydrogen atoms as a function of Ar, He and Xe concentrations [ $H_2(x \text{ sccm}); \text{ Ar, He, Xe } (y=1-x \text{ sccm})$ ] is shown in Fig. 11. A pure hydrogen plasma at 150 mTorr with a 20 sccm flow rate is produced at a coupled rf

power level of 200 W. The corresponding thermal energy of the fast hydrogen atoms in this hydrogen plasma is  $\sim 13\text{-}15$  eV. Noble gases are introduced into the plasma chamber and the total chamber pressure and flow rate are maintained at 150 mTorr and 20 sccm, respectively, by adjusting the hydrogen and noble gas flow rates. As shown in Fig. 11, the average hot thermal energy of the hydrogen atom, obtained from symmetric emission profiles, increases from  $\sim 13\text{-}15$  eV to 25-30 eV as the Ar and He fraction is increased. In contrast, the average energy of the hydrogen atom decreases from 14 eV with an increasing concentration of Xe.

Figures 12 and 13 show the energy and fractional population of fast hydrogen atoms in Ar/H<sub>2</sub> (95/5%) plasmas as the chamber pressure is varied from 10 mTorr to 10 Torr. Plasma emission is sampled perpendicular to the field between the electrodes and along the field lines through holes in the powered and grounded electrodes. As shown in the figures, the fast hydrogen energy (20-25 eV) and their fractional population (70-80%) in  $n=3$  states remains nearly constant as the gas pressure is varied over three orders of magnitude. Very similar profiles of fast hydrogen energy (Fig. 14) and fractional population (Fig.15) as a function of pressure are obtained for (50/50%) He/H<sub>2</sub> plasmas.

The presence of hot hydrogen far away from the high field sheath region is in contradiction with the Collisional Model. The plasma emission is sampled at Positions 1 and 3 (Fig. 2) and the angular variation is obtained by rotating the optical probe. The reference is normal to the chamber axis and as the observation angle is varied, plasma emission far away ( $\sim 6$  cm) from the electrode region is sampled. As shown in Fig. 16, there is a very small influence of the tilt angle on the hot hydrogen energy for both Ar/H<sub>2</sub>

and He/H<sub>2</sub> plasmas. It should be noted here that the symmetry of the emission profile is independent of the angle of observation.

## V DISCUSSION

The observations and implications resulting from this study substantially contradict the Collisional Model [5]. This model argues that excessive H<sub>α</sub> broadening in pure hydrogen and mixtures of hydrogen with noble gases is explained primarily in terms of energetic ions (H<sup>+</sup>, H<sub>2</sub><sup>+</sup> and H<sub>3</sub><sup>+</sup>) accelerated in the cathode fall region followed by energy transfer to the matrix gas (H and H<sub>2</sub>) through charge exchange collisions. The character of atomic hydrogen broadening, namely the fast component temperature and the fractional population of the fast hydrogen atoms is quite different for different gas mixtures. In all variations of the collisional model [5], one consistent aspect is that the energy required for selective heating of the hydrogen atoms in plasmas consisting of hydrogen and hydrogen admixed with other gases is locally absorbed by ions from the electric field in the cathode fall region.

We summarize the significant results of our experimental observations that are inconsistent with the field acceleration based Collisional Model [5]: 1) Hot hydrogen atoms are observed only for pure hydrogen and specific mixtures such as Ar/H<sub>2</sub> and He/H<sub>2</sub> plasmas. 2) In the Ar/H<sub>2</sub> and He/H<sub>2</sub> cases, energy is transferred selectively to hydrogen atoms (15-40 eV) where molecular hydrogen and the admixed gas atoms remain much colder (<0.5 eV) than kinetic energy equilibration [ $(M_H/M_{Ar})^{1/2}$ ;  $(M_H/M_{He})^{1/2}$ ] would provide. 3) The population of neutral H atoms is much hotter (15-40 eV) than any of the bulk species ( $T_{\text{ebulk}} \sim 2-3$  eV in capacitive discharges). 4) The emission profile is symmetric over a wide pressure and mean free path range (three

orders-of-magnitude) and is independent of the observation angle relative to the electric field direction, even for pin shaped electrodes that minimize ion sheath backscatter processes. 5) Comparably hot hydrogen atoms are observed in field-free regions far away (up to 15 cm for the 1 cm spaced capacitive rf system) from the high-field sheath region. In the following section we discuss the inconsistency of the field acceleration based Collisional Model to account for these results.

Let us consider the presence of hot hydrogen atoms that occur only for pure hydrogen and hydrogen admixed with Ar and He plasmas and the absence of hot hydrogen atoms in electronically similar Xe/H<sub>2</sub> plasmas for the entire pressure range from 10 mTorr to 10 Torr. In the field acceleration based Collisional Model, the energy of hot hydrogen atoms should be independent of the nature of the electronically similar background gas except for differing collision cross sections of their ions with H. In order to test the collisional effect of background gases, we consider the cross section data for Balmer alpha and beta line emission from H and H<sup>+</sup> impact reactions on hydrogen (H<sub>2</sub>) and our other reacting gases [37-42]. It should be noted that cross-section data for low energy (< 100 eV) H and H<sup>+</sup> impacting on the reacting gases considered in this paper are not available. Therefore, H<sub>α</sub> emission cross-sections from the impact of 100 eV H atoms on H<sub>2</sub> and noble gas targets  $H + X (X = Ar, He, Xe, H_2) \rightarrow H_\alpha$  are considered. These are  $7 \times 10^{-17} \text{ cm}^2$ ,  $2 \times 10^{-18} \text{ cm}^2$ ,  $5 \times 10^{-18} \text{ cm}^2$  and  $2 \times 10^{-18} \text{ cm}^2$  for Ar He, Xe, and H<sub>2</sub> respectively [38,40,42]. Similarly, the H<sub>α</sub> emission cross-sections from 100 eV H<sup>+</sup> impact  $H^+ + X (X = Ar, Xe, H_2, H) \rightarrow H_\alpha$ , are  $7 \times 10^{-19} \text{ cm}^2$ ,  $2 \times 10^{-17} \text{ cm}^2$ ,  $4 \times 10^{-17} \text{ cm}^2$ , and  $3 \times 10^{-15} \text{ cm}^2$  for Ar, Xe, H<sub>2</sub> and H targets, respectively [37, 39]. The emission cross-section data for the  $H^+ + He \rightarrow H_\alpha$  reaction is not available for H<sup>+</sup> energies below 1.25

keV because of the small magnitude of the photon signals [37]. The cross section for  $H^+ + He \rightarrow H_\alpha$  collisions at  $H^+$  energies of 1.25 keV is given as  $0.6 \pm 0.3 \times 10^{-20} \text{ cm}^2$  and it will be much smaller for lower  $H^+$  energies [37].

The CM argues that  $H^+$  ions will travel and be accelerated over longer distances and gain more energy before interacting with the target gas if the cross-section of  $H^+$  impact on the target gas is lower. As a result, increasingly energetic  $H^+$  ions and, therefore via charge exchange, more energetic H atoms should be observed when the target gas composition is changed from pure hydrogen to  $H_2/Xe$  to  $H_2/Ar$  to  $H_2/He$ . Hence, following these arguments, we should observe the most energetic H atoms in the presence of He gas at low pressure. However, we observe H atoms of comparable energy (30-40 eV in the DC discharge and 20-25 eV in the capacitive discharge) with either He or Ar as the background gas. The fast H atom energies are only 1-2 eV with 90% Xe in DC discharge even though the collision cross section for the process  $H^+ + Xe \rightarrow H_\alpha$  is almost two-orders-of magnitude smaller than that for  $H^+ + H \rightarrow H_\alpha$  process.

We now consider the observation that the energy is transferred selectively primarily to hydrogen atoms (15-40 eV) whereas the atoms of admixed gases remain cold (<0.5 eV) even when the mass ratios are comparable. In the Collisional Model there are neither preferred ions nor atoms and, therefore, one should observe warm atoms of the admixed gases along with the hot hydrogen atoms. To our knowledge, no measurement has ever been made where warm atoms of admixed gases have been found. In collision dominated plasmas at higher gas pressures where an ion is bound to suffer many collisions with the background gas as it moves towards the cathode and where the mass ratios of the constituent gases are comparable, the presence of correspondingly hot atoms

of admixed gases is inferred from the Collisional Model. Let us consider a He/H<sub>2</sub> plasma at 10 Torr with the electron-neutral collision frequency of  $3 \times 10^{10} \text{ s}^{-1}$  [43]. If in gas mixtures where only a trace amount of hydrogen (~1%) is added to the helium plasma, plasma hydrogen and helium ions will undergo many collisions with the background helium gas as they travel towards the cathode. It should be noted that the recombination rate coefficients of helium and hydrogen ions with energies in the range  $\approx 20\text{-}30 \text{ eV}$  is given by the reactions  $He^+ + e \rightarrow He$  and  $H^+ + e \rightarrow H$ . The two-body recombination rates for these two processes are comparable ( $\alpha_e = 10^{-13} \text{ cm}^3/\text{s}$ ) [44-45]. Therefore, the survival probability of both He<sup>+</sup> and H<sup>+</sup> ions as they travel towards the cathode is comparable. It should be noted, however, that with an atomic mass ratio of 4:1 in helium-atomic hydrogen plasmas, we observe hydrogen atoms with average energies of 30-40 eV whereas helium atoms are cold and have energies less than 0.5 eV (Fig. 10).

As shown in Fig. 16, there is a significant presence of comparably hot hydrogen atoms far away from the high-field plasma sheath regions where most of the potential variation occurs. It is well known that outside the sheath region, where the plasma is largely quasi-neutral, the plasma potential variation is very small. Therefore, in a nearly field free region, the field acceleration CM cannot explain the existence of hot hydrogen up to 15 cm from the electrode. In order to explain the presence of hot H atoms in low field regions, the modified CM [5] requires the presence of fast electrons that produce hot atomic hydrogen with an energy comparable in magnitude to that obtained in the high field region where the source of these atoms are accelerated ions in the sheath. The measured thermal electron temperature using the Langmuir probe located between the rf plates, where most of the electron heating takes place, is  $\approx 2\text{-}3 \text{ eV}$  (Table 1) with a

possible small (1 %) fraction of fast electrons. The cross sections for resonant charge exchange transfer ( $Ar_{fast}^+ + Ar_{slow} \rightarrow Ar_{fast} + Ar_{slow}^+$  and  $He_{fast}^+ + He_{slow} \rightarrow He_{fast} + He_{slow}^+$ ) can be utilized to estimate the distance traveled by an ion produced in the cathode fall region without suffering a charge exchange collision that reduces the maximum energy it can obtain. At 20 eV, the resonant charge exchange transfer cross sections ( $\sigma_i$ ) for Ar and He ions are comparable at  $2.2 \times 10^{-15} \text{ cm}^2$  and  $1.5 \times 10^{-15} \text{ cm}^2$ , respectively [46]. The mean free path is given as  $\lambda_i = \frac{1}{n_g \sigma_i} \text{ cm}$ , where  $n_g$ , the neutral particle density, is a function of gas pressure. At 10 mTorr, the mean-free path for charge transfer,  $\lambda_i$ , is 1.3 cm. Therefore, the ions produced in the cathode fall region will not maintain their energy over a distance of 15 cm without suffering a charge exchange collision in these plasmas [46]. These ions cannot be the source of hot H atoms in a region far away from the electrodes. Moreover, the radiative lifetime of the hydrogen n=3 state is  $10^{-8} \text{ s}$  [15] and with an assumed average velocity of  $10^6$ - $10^7 \text{ cm/s}$  corresponding to hydrogen energies of 1-100 eV, it can only travel a distance of 0.1-1 mm before an emission that results in reduced energy. This implies that the observed  $H_\alpha$  emission is a result of local excitation. The rapid thermalization of H atoms with the background gas will also localize fast H concentrations to the region where they are formed. Therefore, a mechanism that explains the localized production of hot H over the larger plasma chamber needs to be developed.

In order to explain the symmetric line emission profile, the CM model mandates the presence of a reflector or divertor. In this model a Gaussian distribution is achieved either by the scattering of hydrogen atoms by the electrode surface or by collisional excitation of  $H_f$  on  $H_2$  with large angle scattering [6], where  $H_f$  represents the hot

hydrogen atoms that have previously collided with the electrode. This implies that the sputtered fast H atoms and the back-reflected fast H atoms from the cathode surface are produced in equal measure to produce a symmetric profile. This requires an “ideal isotropic reflector” to reverse the momentum of a positive ion gained from the electric field to give rise to fast H leaving the cathode in the same abundance as that moving towards the cathode. In addition, according to their model, a “divertor” must also exist such that the ratio of fast H at any given energy towards and away from the cathode remains equal and this must be the case in all directions including the direction perpendicular to the electric field. The interaction of an H atom with a metal surface is quasi-elastic for a large range of targets and energies. The particle and energy reflection coefficients for hydrogen atoms to be reflected back in the energy range of 20-30 eV are only 50% [47]. Therefore, the possibility that backscattered H atoms produced with a comparable distribution to those of the incident H atoms with comparable energy distributions so as to yield a symmetric profile is questionable. In addition, it is well known in plasmas that the effective cross section for many small-angle ion-neutral collisions to produce an equivalent deflection is larger than that for single large-angle collision [46]. Hence, this argument is not viable as a mechanism to explain the symmetry of the plasma emission profile, especially for the DC pin electrode configuration at lower pressures where the tapered tip does not admit a substantial axial backscattered H atomic component.

Electron-ion, electron-neutral, and ion-neutral collision frequencies are a complex function of not only the gas pressure but also of the energy of the colliding particles. Therefore, in order to obtain better insight into the energy transfer through the collision

and charge exchange processes, an estimate of the collision frequencies at the pressures and energies of interest is discussed. For a flux of incident electrons with velocities  $v$  colliding with a background neutral gas, the collision frequency is given approximately as  $\nu_{en} = n_g \sigma v = n_g K \sim 3 \times 10^9 \times P(\text{Torr}) \text{s}^{-1}$  where  $n_g$  is the neutral number density given by Loschmidt's number and  $\sigma$  is the collision cross-section and  $K$  is the rate constant [48-49]. At 10 mTorr and 10 Torr, the electron-neutral collision frequencies are  $3 \times 10^7 \text{ s}^{-1}$  and  $3 \times 10^{10} \text{ s}^{-1}$ , respectively, a variation of three orders of magnitude. Therefore, at 10 mTorr the electron-neutral collision frequency is comparable to the rf frequency and a typical electron can travel to the anode in one rf period of 73 ns. The LP measured bulk electron temperature is 2-3 eV and the electron can travel a distance of about 8 cm during one rf period without suffering collisions with the background neutral gas. Therefore, in low-collision-rate plasmas (10 mTorr) compared to the ion transit time between the electrodes, based on the CM, fast H atoms produced by the charge exchange process will dominantly scatter in the direction of the accelerated ions and will yield a predominant red or blue wing in the emission spectrum relative to the direction of observation. However, the data presented in this paper are contrary to the prediction of the CM field acceleration mechanism of energy transfer to hydrogen atom. The symmetric line profile is independent of the angle of observation.

## VI. CONCLUSION

The mechanism of extraordinary broadening of the hydrogen Balmer lines in hydrogen admixed with noble gases has been studied. It is concluded that, substantial additional measurements of  $H_\alpha$  broadening including observations of the different hydrogen species

concentrations in the sheath region as well as away from it are required. A more thorough reexamination and further development of a theory for  $H_{\alpha}$  broadening for the wide range of plasma conditions examined in this and other works is required to more fully understand this curious and potentially useful process.

References:

1. A.L. Cappelli, R.A. Gottscho, and T.A. Miller, "Doppler-broadened line shapes of atomic hydrogen in a parallel-plate radio frequency discharge," *Plasma Chem. Plasma Process*, vol. 5, pp. 317-331, 1985.
2. G. Baravian, Y. Chouan, A. Ricard, and G. Sultan, "Doppler broadened  $H_{\alpha}$  line shapes in a rf low pressure  $H_2$  discharge," *J. Appl. Phys.*, vol. 61, pp. 5249-5253, 1987.
3. S. Djurovic and J.R. Roberts, "Hydrogen Balmer alpha line shapes for hydrogen-argon mixtures in a low-pressure rf discharge," *J. Appl. Phys.*, vol. 74, pp. 6558-6565, 1993.
4. C. Barabeau and J. Jolly, "Spectroscopic investigation of energetic atoms in a DC hydrogen glow discharge," *J. Phys. D, Appl. Phys.*, vol. 23, pp. 1168-1174, 1990.
5. N. Cvetanovic, M. M. Kuraica, and N. Konjevic, "Excessive Balmer line broadening in a plane cathode abnormal glow discharge in hydrogen," *J. Appl. Phys.*, vol. 97, pp. 33302-33309, 2005.
6. M.R.G. Adamov, B.M.Obradovic, M.M. Kuracia, and N. Konjevic, "Doppler spectroscopy of hydrogen and deuterium Balmer alpha line in an abnormal glow discharge," *IEEE Trans. Plasma Sci.*, vol. 31, no. 3, pp. 444-454, 2003.
7. E. L. Ayers and W. Benesch, "Shapes of atomic-hydrogen lines produced at cathode surface," *Phys. Rev. A, Gen. Phys.*, vol. 37, pp. 194, 1988.
8. W. Benesch and E. Li, "Line shapes of atomic hydrogen in hollow cathode discharge," *Opt. Lett.*, vol. 9, no. 8, pp. 338-340, 1984.
9. M. Kuraica and N. Konjevic, "Line shapes of atomic hydrogen in a plane-cathode

- abnormal glow discharge,” *Phys. Rev. A*, vol. 46, no. 7, pp. 4429-4432, 1992.
10. M. Kuraica, N. Konjevic, M. Platisa, and D. Pantelic, “Plasma diagnostics of the Grimm-type glow discharge,” *Spectrochim. Act*, vol. 47, pp. 1173, 1992.
  11. S. Alexiou and E. Leboucher-Dalimier, “Hydrogen Balmer- $\alpha$  in dense plasmas,” *Phys. Rev. E*, vol. 60, no. 3, pp. 3436-3438, 1999.
  12. S. B. Radovanov, J. K. Olthoff, R. J. Van Brunt, and S. Djorovic, “ Ion kinetic-energy distribution of Balmer-alpha ( $H_{\alpha}$ ) excitation in Ar- $H_2$  radio-frequency discharges,” *J. Appl. Phys.*, vol. 78, pp. 746-757, 1995.
  13. A. V. Phelps, “Collisions of  $H^+$ ,  $H_2^+$ ,  $H_3^+$ ,  $ArH^+$ ,  $H^-$ ,  $H$ , and  $H_2$  with Ar and of  $Ar^+$  and  $ArH^+$  with  $H_2$  for Energies from 0.1 eV to 10 keV,” *J. Phys. Chem. Ref Data*, vol. 21, pp. 883-897, 1992.
  14. S. B. Radovanov, K. Dzierzega, J. R. Roberts, and J. K. Olthoff, “Time resolved Balmer-alpha emission from fast hydrogen atoms in low pressure, radiofrequency discharges in hydrogen,” *Appl. Phys. Lett.*, vol. 66, no. 20, pp. 2637-2639, 1995.
  15. A. Bogaerts and R. Gijbels, “Effects of adding hydrogen to an argon glow discharge: Overview of some relevant processes and some quantitative explanations,” *J. Anal. At. Spectrom.*, vol. 15, pp. 441-449, 2000.
  16. R. L. Mills, P. Ray, B. Dhandapani, R. M. Mayo, and J. He, “Comparison of excessive Balmer  $\alpha$  line broadening of glow discharge and microwave hydrogen plasmas with certain catalysts,” *J. Appl. Phys.*, vol. 92, pp.7008-7022, 2002.
  17. R. L. Mills, P. C. Ray, M. Nansteel, X. Chen, R.M. Mayo, J. He, and B. Dhandapani, “Comparison of excessive Balmer  $\alpha$  line broadening of inductively and capacitively coupled RF, microwave, and glow discharge hydrogen plasma with

- certain catalysts”, *IEEE Trans. Plasma Sci.*, vol. 31, pp. 338-355, 2003.
18. R. L. Mills and P. Ray, “Extreme ultraviolet spectroscopy of helium-hydrogen plasma,” *J. Phys. D: Appl. Phys.*, vol. 36, pp. 1535-1542, 2003.
  19. R. L. Mills, P. Ray, B. Dhandapani, M. Nansteel, X. Chen, and J. He, “ New power source from fractional quantum energy levels of atomic hydrogen that surpasses internal combustion,” *J Mol. Struct*, vol. 643, no. 1-3, pp. 43-54, 2002.
  20. R. Mills and P. Ray, “Spectral emission of fractional quantum energy levels of atomic hydrogen from a helium-hydrogen plasma and the implications for dark matter,” *Int. J. Hydrogen Energy*, vol. 27, no. 3, pp. 301-322, 2002.
  21. C. Chen, T. Wei, L. R. Collins, and J. Phillips, “Modelling the discharge region of a microwave generated hydrogen plasma.” *J. Phys. D: Appl. Phys.*, vol. 32, pp. 688-698, 1999.
  22. R. Mills, M. Nansteel, and P. Ray, “Argon-hydrogen-strontium discharge light source,” *IEEE Trans. Plasma Sci.*, vol. 30, no. 2, pp. 639-652, 2002.
  23. R. Mills, M. Nansteel, and P. Ray, “Bright hydrogen-light source due to resonant energy transfer with strontium and argon ions”, *New J. Phys.*, vol. 4, pp. 70.1-70.28, 2002.
  24. R. Mills, “Spectroscopic identification of a novel catalytic reaction of atomic hydrogen and hydride ion product”, *Int. J. Hydrogen Energy*, vol. 26, pp. 1041-1058, 2001.
  25. R. Mills and P. Ray, “Vibrational spectral emission of fractional-principal-quantum-energy-level hydrogen molecular ion, *Int. J. Hydrogen Energy*, vol. 27, pp. 533-564, 2002.

26. R. Mills, "Classical Quantum Mechanics", Physics Essays, Vol. 16, No. 4, pp. 433-498, 2003.
27. National Institute of Standard and Technology, Physical Reference Data,  
<http://physics.nist.gov/PhysRefData/PerTable/index.html>
28. Hans R. Griem, Principles of Plasma Spectroscopy, p. 193, Cambridge University Press, NY (1997)
29. W.L. Wiese, "Line Broadening", in Plasma Diagnostic Techniques, R. H. Huddleston and S. L. Leonard, Eds., Academic Press, NY, (1965)
30. F. F. Chen, "Electric Probes", in Plasma Diagnostic Techniques, R. H. Huddleston and S. L. Leonard, Eds., Academic Press, NY, (1965).
31. S. M. Tysk, C. M. Denning, J.E. Scharer, and K. Akhtar, "Optical, wave measurements, and modeling of helicon plasmas for a wide range of magnetic fields," Physics of Plasmas, Vol. 11, pp. 878, 2004.
32. A. Ganguli, M.K. Akhtar, and R.D. Tarey, "Investigation of microwave plasmas produced in a mirror machine using ordinary-mode polarization", Plasma Sources Science & Technol. 8, pp. 519, 1999.
33. V.A. Godyak, "Nonequilibrium EEDF in Gas Discharge Plasma", IEEE Trans. Plasma Sc., vol. 34, pp. 755, 2006.
34. E. Abdel-Fattah and H. Sugai, " Electron heating mode transition observed in a very high frequency capacitive discharge", App. Phys. Lett., Vol. 83, 8, pp. 1533, 2003.
35. C.M.O. Mahnoy, P. D. Maguire, and W.G. Graham, " Electrical characterization of radiofrequency discharges", Plasma Sources Sci Technol., Vol. 14, pp. S60 (2005).
36. A. Zecca, G.P. Karwasz, and R.S. Brusa, "One century of experiments on electron-

- atom and molecule scattering: a critical review of integral cross-sections. Atoms and diatomic molecules”, *Il Nuovo Cimento*, Vol. 19, No. 3, pp. 1-146, 1996
37. B. Van Zyl, M. W. Gealy, and H. Neumann, “Balmer-line emission from low-energy  $H^+$  impact on rare-gas atoms”, *Phys. Rev. A* , Vol. 33, 4, pp. 2333, 1986.
  38. B. Van Zyl, H. Neumann, H.L. Rothwell, Jr., and R.C. Amme, “Balmer- $\alpha$  and Balmer- $\beta$  emission cross sections for  $H + Ar$  collisions”, *Phys. Rev. A* , Vol. 21, pp. 716, 1980.
  39. B. Van Zyl, H.L. Rothwell, Jr., and H. Neumann, “Balmer- $\alpha$  and Balmer- $\beta$  emission cross sections for  $H^+ + Ar$  collisions”, *Phys. Rev. A* , Vol. 21, pp. 730, 1980.
  40. B. Van Zyl, M. W. Gealy, and H. Neumann, “ Balmer- $\alpha$  and Balmer- $\beta$  emission cross sections for low-energy H collisions with He and  $H_2$ ”, *Phys. Rev. A*, Vol. 28, pp. 176, 1983.
  41. B. Van Zyl, M. W. Gealy, and H. Neumann , “Excitation of low-energy H atoms in  $H+Ne$  collisions”, *Phys. Rev. A* , Vol. 31, 5, pp. 2922, 1985.
  42. B. Van Zyl, H. Neumann, and M. W. Gealy, “Balmer-line emission from low-energy H impact on Kr and Xe”, *Phys. Rev. A* , Vol. 33, pp. 2093, 1986.
  43. Kamran Akhtar, John E. Scharer, Shane Tysk and Enny Kho,” Plasma interferometry at high pressures”, *Rev. Sci. Instrum.*, 74, pp. 996, 2003.
  44. M. Arnaud and R. Rohenflug, *Astron. & Astrophys. Suppl.* 60, 425 (1985),
  45. T. Kato and E. Asano, “ comparison of recombination rate coefficients given by empirical formulas for ions from hydrogen through nickel”, NIFS-DATA-54, National Institute of Fusion Science (NIFS), Nagoya, Japan, 1999.
  46. E.W. McDaniel, J.B.A. Mitchell, and M.E. Rudd, *Atomic Collision: Heavy Particles*

Projectiles, Wiley, New York, 1993.

47. D.E. Post and R. Behisch, Physics of Plasmas-Wall Interactions in Controlled Fusion, NATO ASI series B, 131, 423, (1986)
48. M.A. Lieberman and A.J. Lichtenberg, "Principles of plasma discharges and material processing", 2<sup>nd</sup> edition, Hoboken, New Jersey: John Wiley & Sons, Inc., 2005.
49. V. Vahedi, R. A. Stewart, and M. A. Lieberman, "Analytic model of the ion angular distribution in a collisional sheath," *J. Vac. Sci. Technol. A*, vol. 11, pp. 1275-1282, 1993.

TABLE 1

Langmuir probe measurement of plasma density and electron temperature in capacitively coupled radio frequency plasmas at 100 mTorr and 100 W coupled rf power.

Gas Composition	Bulk Plasma Density ( $\text{cm}^{-3}$ )	Bulk Electron Temperature (eV)
Ar	$2-3 \times 10^{10}$	2.1-2.4
Ar/10%H <sub>2</sub>	$5-8 \times 10^9$	1.8-2.0
He	$6-9 \times 10^9$	2.5-3.0
He/10%H <sub>2</sub>	$3-5 \times 10^9$	1.9-2.3
Xe	$2-5 \times 10^{10}$	1.7-2.0
Xe/10%H <sub>2</sub>	$7-9 \times 10^9$	1.7-1.9

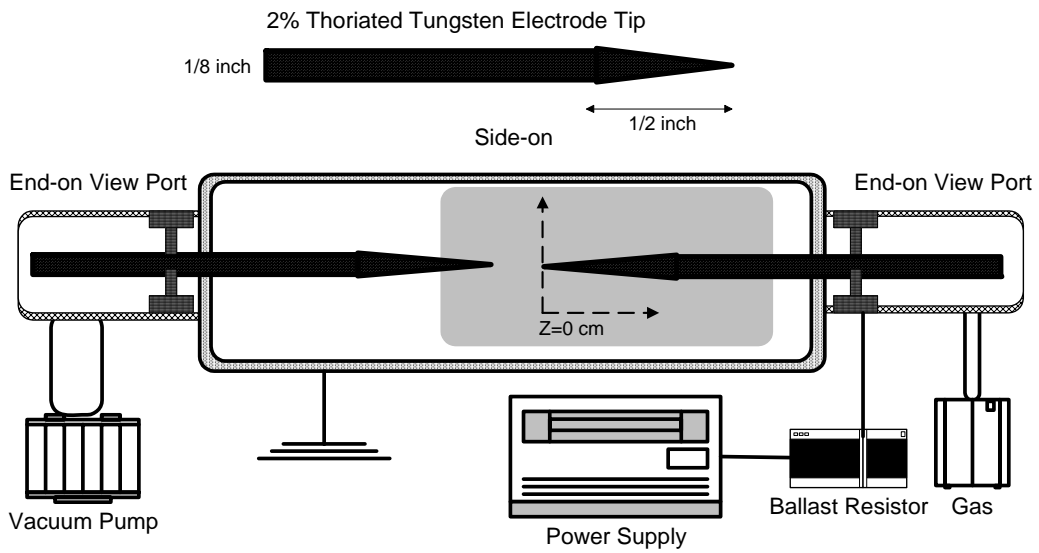


Fig 1. Schematic of the DC discharge created between the fine tips of 2% thoriated tungsten electrodes with the direction of axial scans defined. The cathode tip is taken as  $z=0$  cm for side-on observations measured along the axis of the cathode from its tip to its electrical connection.

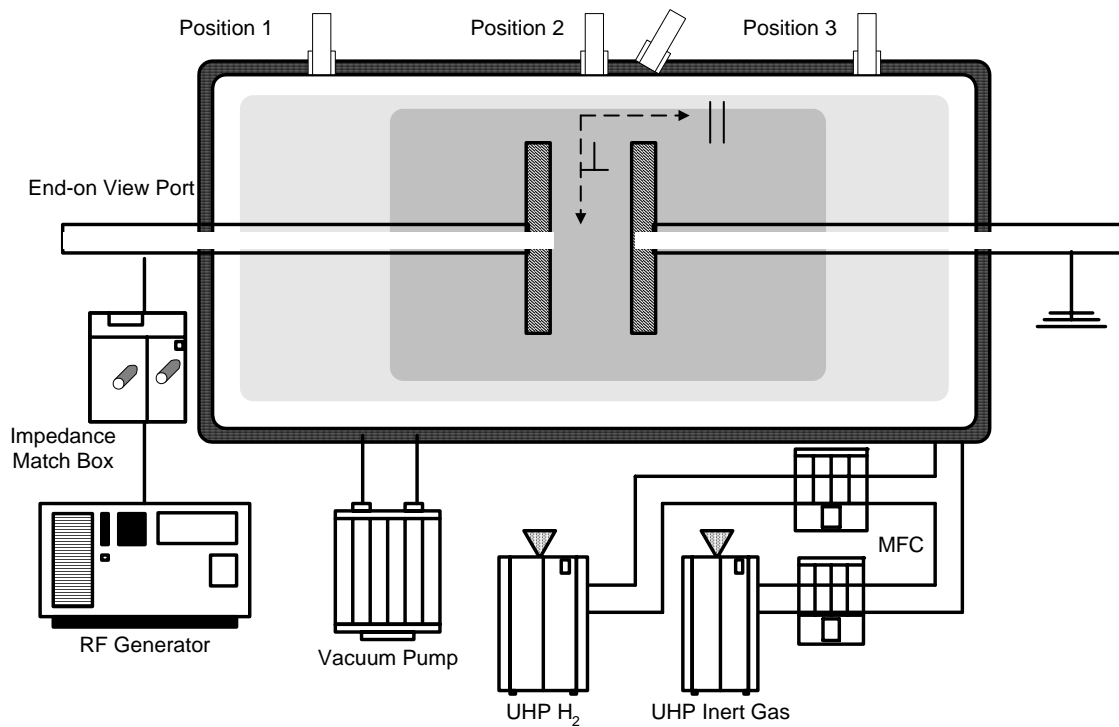


Fig. 2. Schematic of the capacitively coupled radio frequency plasma system. Optical emission spectroscopy is performed perpendicular to the electric field (Position 2) and parallel to the field (end-on observation).

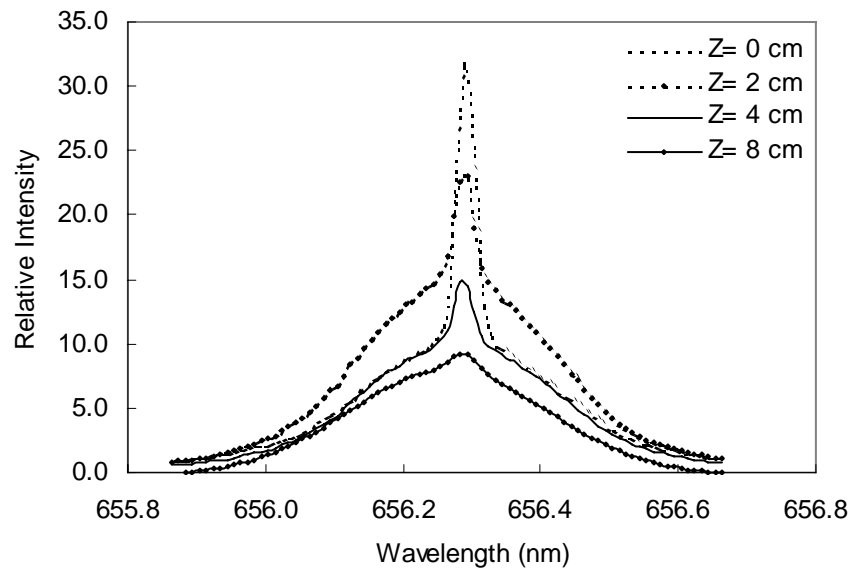


Fig. 3. Axial scan of the 656.3 nm Balmer  $\alpha$  line width recorded on a 1 Torr  $Ar/H_2$  (95/5%) DC plasma discharge with needle-like electrodes at 400 V and 20 mA showing 80% of the hydrogen was 'hot' with an average hydrogen atom energy of 40 eV, compared to  $< 0.5$  eV for the slow population.

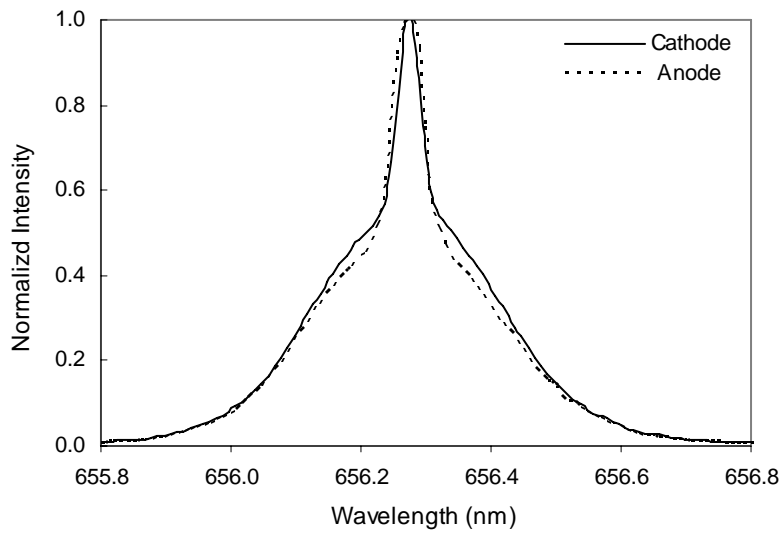


Fig. 4. The 656.3 nm Balmer  $\alpha$  line width recorded end-on (parallel to the electric field) on a 1 Torr  $Ar/H_2$  (95/5%) DC plasma discharge with needle-like electrodes at 400 V and 20 mA. Both views looking towards the cathode as well as the anode show a symmetrical emission profile. The temperature of hot hydrogen atoms is in the range of 38-40 eV.

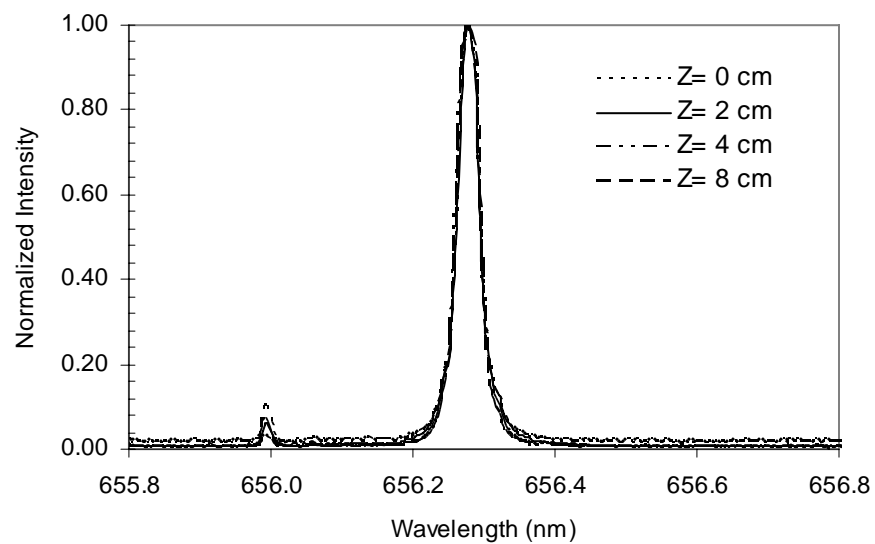


Fig. 5. Axial scan of the 656.3 nm Balmer  $\alpha$  line width recorded on a 1 Torr Xe /H<sub>2</sub> (95/5%) DC plasma discharge with needle-like electrodes at 400 V and 20 mA showing only a cold population of <1 eV with a decrease in intensity along the cathode due to a decrease in electron density and energy.

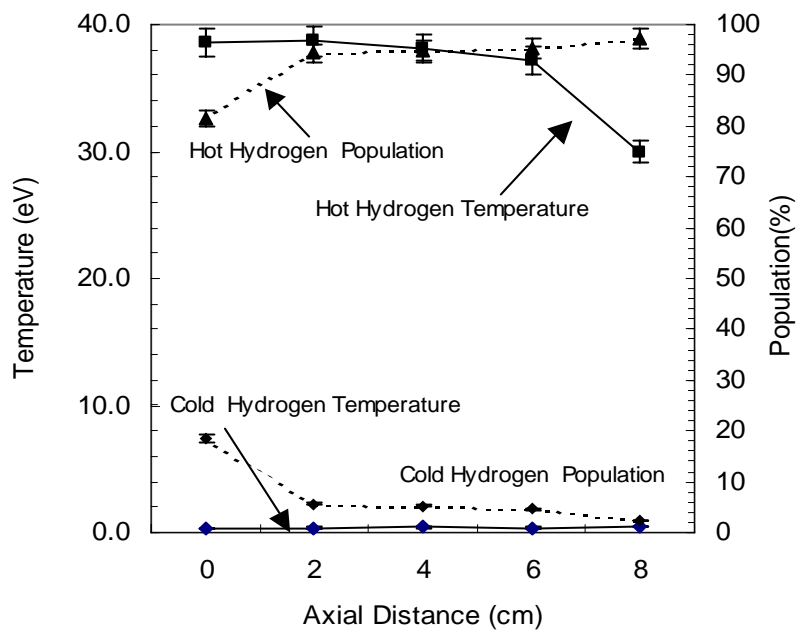


Fig. 6. Axial plots of hot hydrogen atoms temperature and population (given by area under the curve) corresponding to the spectrum in Figure. 3. A hot hydrogen population is present even at a distance of 8 cm away from the cathode tip where most of the potential falls.

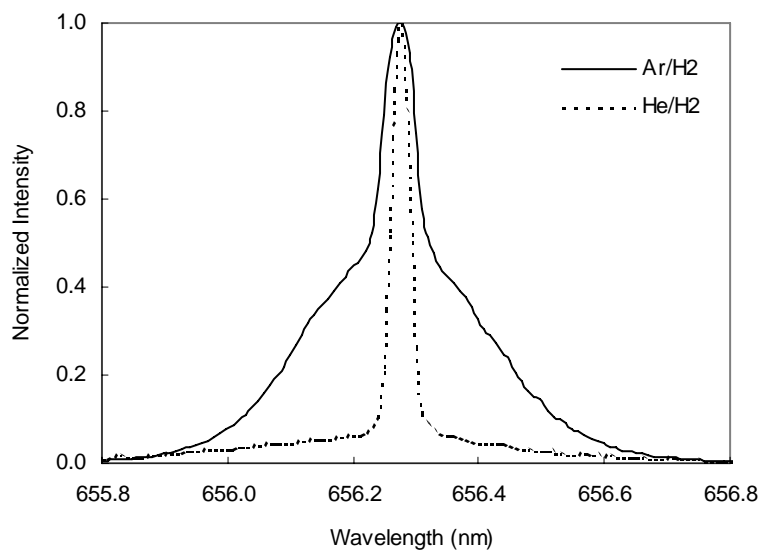


Fig. 7 Normalized end-on emission spectrum of 1 Torr Ar/5% $H_2$  and He/5% $H_2$  plasma looking towards the anode. Note the symmetrical emission profile.

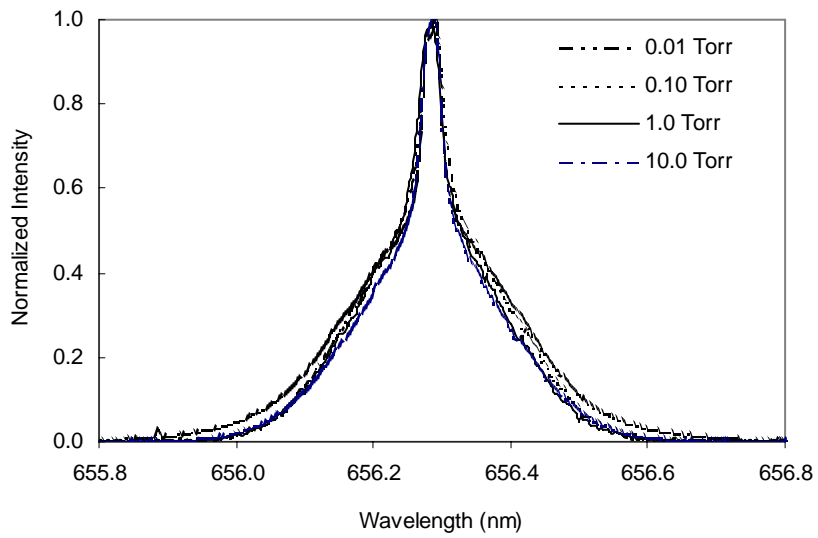


Fig. 8 There is very little variation in the normalized end-on emission spectrum of Ar/5% $H_2$  plasma looking towards cathode as the gas pressure is varied over three-orders-of-magnitude from 10 mTorr to 10 Torr. Note the symmetrical emission profile.

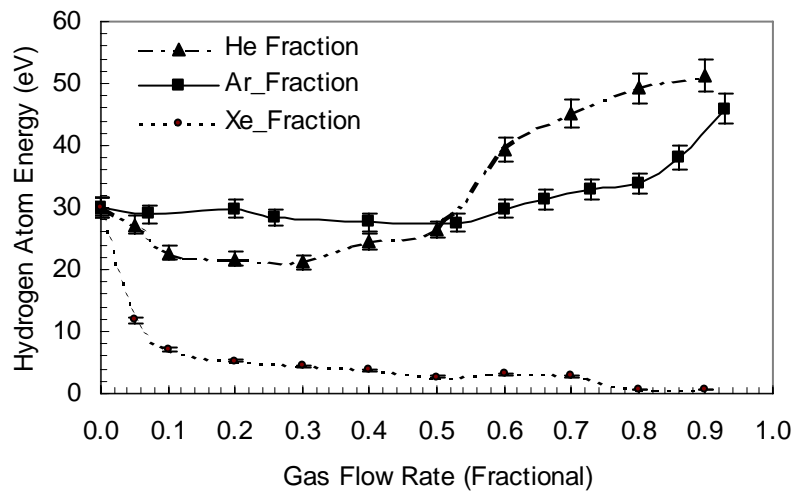


Fig.9 Energy of hot hydrogen atoms as a function of fractional concentration of admixed gases in a DC discharge at 100 mTorr. Note the increase in the energy of hot H as Ar and He concentration increases and decrease in energy with the addition of Xe.

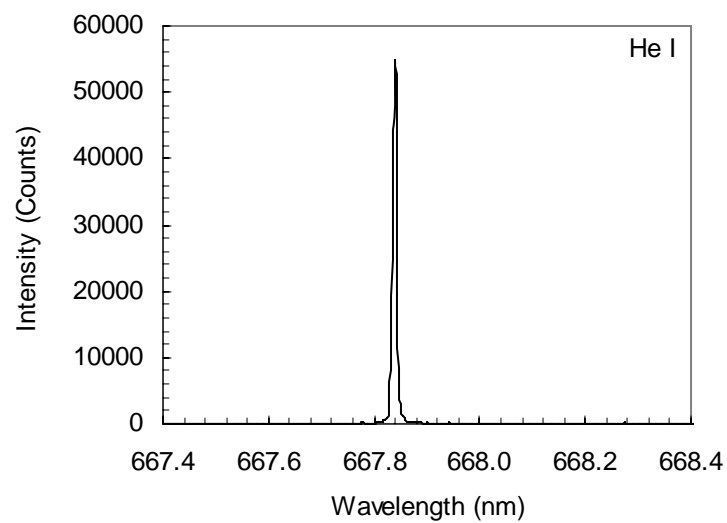


Fig. 10

Fig. 10 The 667.816 nm He I line width for 1 Torr He/H<sub>2</sub> (95/5%) at 400 V and 20 mA .  
No broadening was observed,

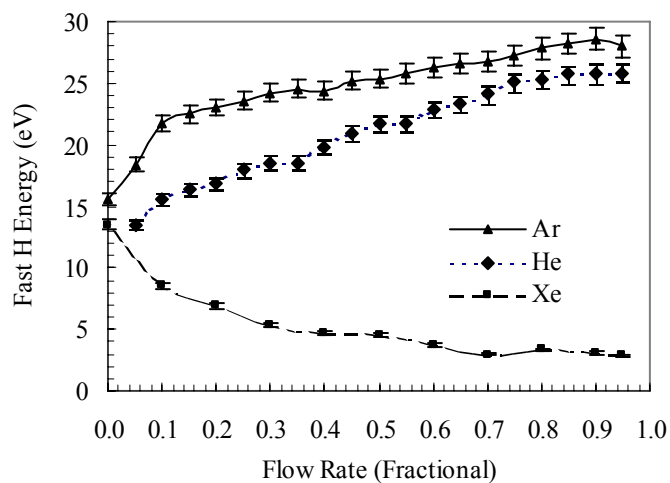


Fig.11. Energy of hot hydrogen atom in Ar/H<sub>2</sub>, He/H<sub>2</sub> and Xe/H<sub>2</sub> plasmas as a function of the noble gas concentration [H<sub>2</sub>(x) Ar, He, Xe(y=1-x)] in capacitively coupled rf discharge. The plasma chamber is maintained at 150 mTorr with a total flow rate of 20 sccm. The coupled rf power is 200 Watt. H<sub>α</sub> emission is sampled perpendicular to the electric field between the capacitive plates.

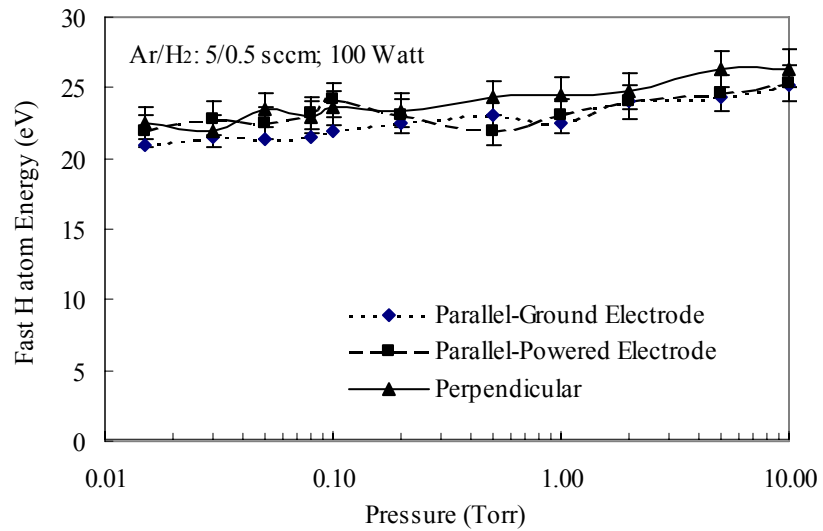


Fig. 12: Hot hydrogen atom temperature for capacitively coupled Ar/H<sub>2</sub> discharge at different gas pressures. Observations are made perpendicular to the field between the electrodes and parallel to the field lines through holes in both powered and grounded electrodes.

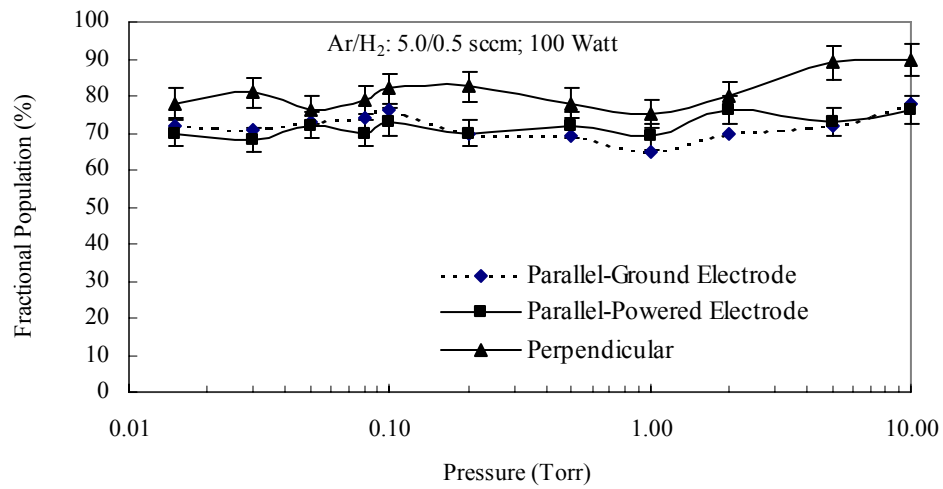


Fig.13. Fractional population of hot hydrogen atoms in  $n=3$  excited state in a capacitively coupled Ar/H<sub>2</sub> discharge at different gas pressures.

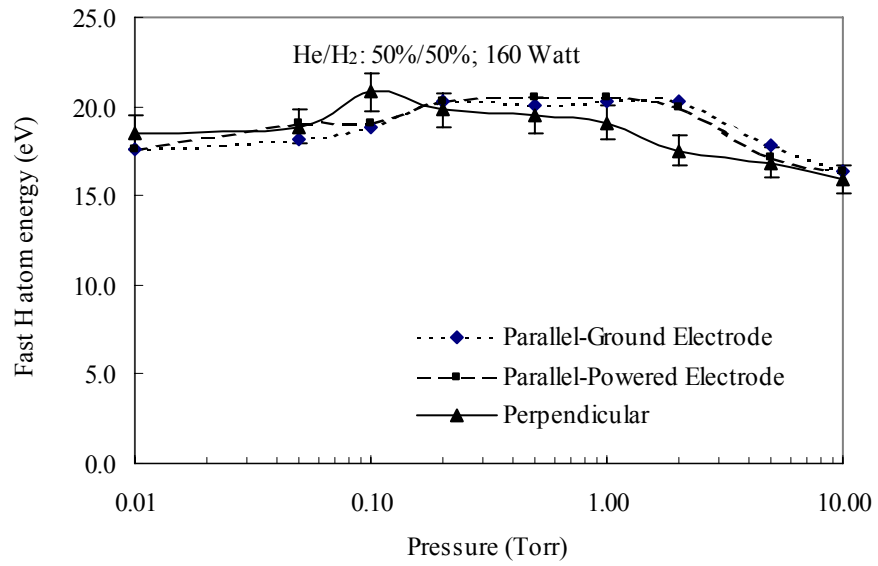


Fig.14. Hot hydrogen atom energy in a capacitively coupled He/H<sub>2</sub> discharge at different gas pressures.

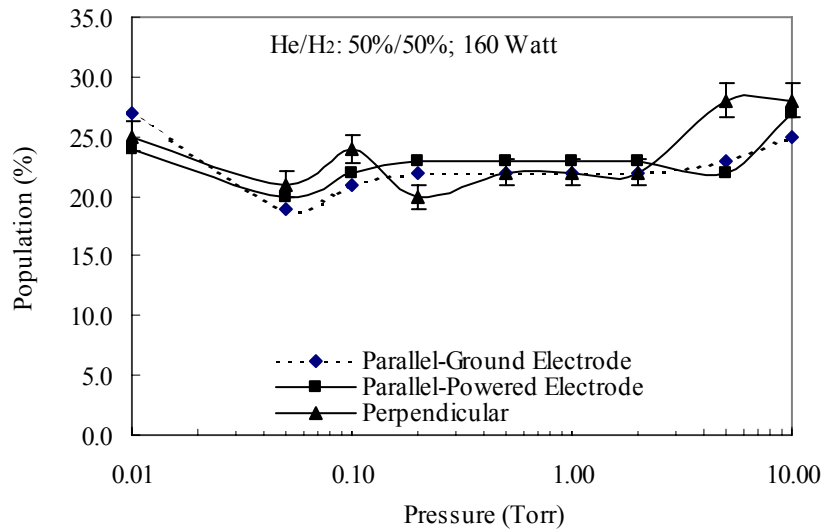
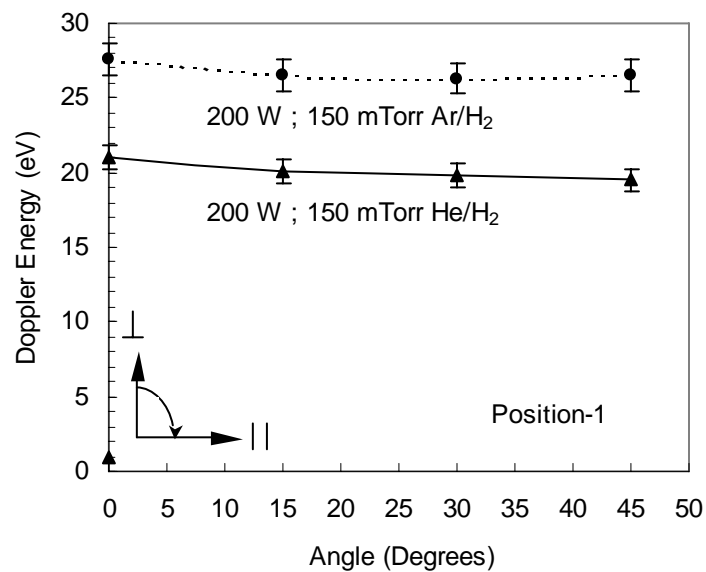
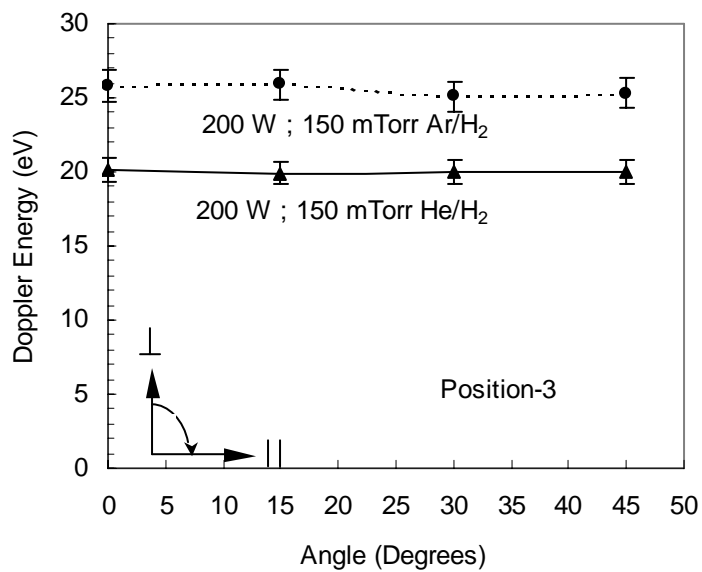


Fig.15. Fractional population of hot hydrogen atoms ( $n=3$  state) in a capacitively coupled He/H<sub>2</sub> discharge at different gas pressures.



(a)



(b)

Fig.16. Angular variation of Doppler energy of hot hydrogen atom in a capacitively coupled radio frequency discharge at 150 mTorr 50%Ar/50%H<sub>2</sub> and 50%He/50%H<sub>2</sub> plasma at 200 W. Plasma emission is sampled at Position 1 (Fig. a) and Position 3 (Fig. b) far away from the region of high field in plasma sheath. Reference is normal to the chamber axis.